FEBS Letters 581 (2007) 5099–5104

Phenotypic behavior of C2C12 myoblasts upon expression of the dystrophy-related caveolin-3 P104L and TFT mutants

Alessandro Fanzani[a,*], Elena Stoppani[a], Laura Gualandi[b], Roberta Giuliani[a], Ferruccio Galbiati[c], Stefania Rossi[a], Anna Fra[d], Augusto Preti[a], Sergio Marchesini[a]

[a] *Department of Biomedical Sciences and Biotechnology, Unit of Biochemistry, University of Brescia, Viale Europa 11, 25123 Brescia, Italy*
[b] *Department of Biomedical Sciences and Biotechnology, Unit of General Pathology, University of Brescia, Italy*
[c] *Department of Pharmacology, University of Pittsburgh School of Medicine, Pittsburgh PA, USA*
[d] *Department of Biomedical Sciences and Biotechnology, Unit of Pathology and Immunology, University of Brescia, Italy*

Received 25 June 2007; revised 19 September 2007; accepted 26 September 2007

Available online 4 October 2007

Edited by Horst Feldmann

Abstract **Caveolin-3 (Cav-3) is the main scaffolding protein present in myofiber caveolae. We transfected C2C12 myoblasts with dominant negative forms of Cav-3, P104L or ΔTFT respectively, which cause the limb-girdle muscular dystrophy 1-C. Both these forms triggered Cav-3 loss during C2C12 cell differentiation. The P104L mutation reduced myofiber formation by impaired AKT signalling, accompanied by dramatic expression of the E3 ubiquitin ligase Atrogin. On the other hand, the ΔTFT mutation triggered hypertrophic myotubes sustained by prolonged AKT activation, but independent of increased levels of follistatin and interleukin-4 expression. These data suggest that separated mutations within the same dystrophy-related gene may cause muscle degeneration through different mechanisms.**

Keywords: Caveolin 3; Dystrophy; AKT; Follistatin; NFATC2; IL-4; Murf-1; Atrogin

1. Introduction

Caveolin 3 (Cav-3) is a muscle-specific scaffolding protein which recruits lipids and several signalling and structural proteins in caveolae [1–3]. Cav-3 expression occurs normally during myofiber differentiation and hypertrophy through activation of both p38 and PI3-kinase/AKT pathways [4,5], whereas its expression results down-regulated during atrophy, suggesting its role causally linked to myofiber maturation [5].

Different human Cav-3 mutations have been characterized to cause four muscle disease phenotypes, including limb-girdle muscular dystrophy, rippling muscle disease, distal myopathy and hyperCKemia [3]: most of these mutations give rise to dominant negative forms which oligomerize with the wild type Cav-3, leading to protein loss. In particular, two heterozygous mutations were first identified within the Cav-3 gene as responsible of the autosomal dominant limb-girdle muscular dystrophy 1-C (LGMD-1C) [6], consisting of a 9-bp microdeletion (ΔTFT) in the caveolin-scaffolding domain and a missense mutation (P104L) in the transmembrane domain. These mutated proteins are not properly targeted to plasma membrane, being retained in the Golgi and endoplasmic reticulum compartments, where they form unstable aggregates with wild type Cav-3 undergoing proteosomal degradation [7].

In the last years, many aspects emerged from the characterization of LGMD-1C mutants, underlying that different mechanisms occur during myofiber degeneration induced by loss of Cav-3. In particular, transgenic mice harboring the Cav-3 P104L mutation were characterized by a severe myopathy accompanied by increase of nitric oxide synthase activity and myostatin type I receptor activation [8,9], whereas the expression of P104L caused in zebrafish severe disruption of muscle differentiation [10]. On the other side, myoblasts expressing ΔTFT mutation underwent apoptosis by altered Src localization [11] and resulted more susceptible to oxidative stress by alteration of PI3-kinase signalling [12].

Here we generated C2C12 myoblasts stably transfected with the vectors harboring either the P104L or ΔTFT Cav-3 mutations, demonstrating that these forms differentially affect myoblast differentiation leading to distinct cell behaviors.

2. Materials and methods

2.1. Materials

All the reagents are from Sigma–Aldrich, if not otherwise indicated.

2.2. Cell culture

The mouse C2C12 myoblasts were maintained at subconfluent density at 37°C in 5% CO_2 in Dulbecco's modified Eagle's medium (DMEM) high glucose supplemented with 10% fetal bovine serum (FBS) and 100 μg/ml penicillin–streptomycin. To induce differentiation, confluent cells were shifted to a medium containing DMEM supplemented with 2% horse serum (HS). To quantify the myotube number and diameter, 10 fields were chosen randomly and 10 myotubes were measured per field. The number and the average diameter taken along the length of the myotube were the mean of 10 measurements.

2.3. Stable transfections

C2C12 myoblasts were cotransfected by Lipofectamine 2000 reagent (Invitrogen) with the vector harboring the Cav-3 mutation (pCAGGS-P104L or ΔTFT) in presence of a pcDNA vector conferring the geneticin resistance (0.5 mg/ml).

*Corresponding author. Fax: +39 030 3701157.
E-mail address: fanzani@med.unibs.it (A. Fanzani).

Abbreviations: DMEM, Dulbecco's modified Eagle's medium; FBS, fetal bovine serum; HS, horse serum; MHC, myosin heavy chain; NFATC, nuclear factor of activated T-cells; IL-4, Interleukin 4

0014-5793/$32.00
doi:10.1016/j.febslet.2007.09.055

2.4. Western blot analysis

Cav-3 was detected with a mouse monoclonal antibody (clone 26, BD Transduction Laboratories) in the insoluble membranous fraction obtained upon centrifugation (12 000 × g for 15 min at 4 °C) of the cells harvested in a Triton buffer composed by 10 mM Tris pH 8.0, 0.15 M NaCl, 5 mM EDTA, 1% Triton X-100, protease inhibitors (Roche Molecular Biochemicals). Antibodies for the phosphorylated Ser^{473} of AKT (Cell Signalling), myogenin (Santa Cruz Biotechnology, clone F5D), the phosphorylated form of P70S6K (Cell Signalling) and myosin heavy chain (MHC) (Hybridoma Bank, University of Iowa) were used on cleared extracts from cells harvested in RIPA lysis buffer (20 mM Tris–HCl pH 7.6, 50 mM NaCl, 1% Nonidet P40, 0.5% sodium deoxycholate, 0.1% SDS, protease inhibitors). An antibody against alpha tubulin was used to normalize the loading.

2.5. Semiquantitative RT-PCR analysis

Total RNA was obtained by Tri-reagent extraction, digested with 1 unit of DNAase (DNA-free, Ambion), and retrotranscribed (2 μg) with 400 U of MMLV-RT (Promega). The primers (250 nM) were as follows: follistatin forward primer: 5′-CTCTTCAAGTGGATGATTTTC; reverse: 5′-ACAGTAGGCATTATTGGTCTG; NFATC2 forward primer: 5′-CTTCAGATCTTCATTGGGACAGCA; reverse: 5′-GCAGCTGTCCATGTCTTGTCTCTC; Interleukin 4 (IL-4) forward primer: 5′-TTTCTCGAATGTACCAGGAGCCATA; reverse: 5′-GGACTCATTCATGGTGCAGCTTATC.

2.6. Real-time PCR analysis

Quantitative PCR was performed with a Biorad iCycler iQ™ Real-time PCR Detection System using a iQ™ SYBR Green Supermix (Biorad) according to the manufacturer's instructions. The primers (250 nM) were as follows: Murf-1 forward primer: 5′-GGTGCCTACTTGCTCCTTGT; reverse: 5′-CTGGTGGCTATTCTCCTTGG; Atrogin forward primer: 5′-CGACCTGCCTGTGTGCTTAC; reverse: 5′-CTTGCGAATCTGCCTCTCTG. All PCR reactions were performed in 96-well optical plates (Biorad) containing primers, 8 ng of cDNA, and 10 μl of reaction mix in a total volume of 20 μl. Gene expression levels were normalized to gapdh mRNA expression.

2.7. Statistics

All of the data are expressed as means ± S.E. Statistical significance was determined using *t*-student analysis. A P value of <0.05 was considered significant.

3. Results and discussion

3.1. Expression of Cav-3 mutants differentially affects C2C12 cell differentiation

Among the several mutations occurring within Cav-3 gene, the missense mutation P104L and the tripeptide deletion ΔTFT cause the autosomal dominant form of limb-girdle muscular dystrophy 1-c (LGMD-1C) [6,7].

We generated C2C12 myoblasts stably transfected with either the dominant negative P104L or ΔTFT mutants (LGMD-1C myoblasts), which were tested for transgene expression in proliferating myoblasts (Fig. 1A), whereas endogenous Cav-3 was absent in parental C2C12 cells. As shown in Fig. 1B, as parental C2C12 cells exhibited the normal formation of multinucleated myotubes over a time-course differentiation, both LGMD-1C myoblasts displayed an evident opposite phenotypic behavior: P104L cells showed a severe undifferentiated phenotype, whereas ΔTFT cells formed multigiant myotubes. Western blot analysis (Fig. 1C) showed the gradual increase of Cav-3 expression in differentiating parental cells, whereas protein loss was observed in both LGMD-1C myoblasts, as confirmed by the relative band quantifications. As shown in Fig. 1D (left panel), the myotube number in P104L myoblasts was severely reduced, as very few thin myofibers were observed, while ΔTFT cells maintained the ability to form myotubes, although with a significantly reduced fashion compared to parental cells. Remarkably, the average size of ΔTFT myotubes was increased of about twofold compared to control myofibers (Fig. 1D, right panel). We therefore investigated the molecular mechanisms underlying the phenotype of LGMD-1C myoblasts, first analysing by Immunoblot the time-course expression of both phosphorylated AKT form and myogenin (Fig. 2A), two key markers of myoblast differentiation. As parental cells showed a transient AKT activation, reaching a peak at day 3 paralleled by increased myogenin expression, P104L cells displayed impaired AKT activation accompanied by almost undetectable myogenin expression. On the other side, the behavior of ΔTFT cells was characterized by a long lasting increase of AKT phosphorylation paralleled by increase of myogenin; accordingly, the phosphorylation of the downstream AKT target P70S6K (Fig. 2B) was more sustained in ΔTFT myotubes due to AKT overactivation, while a low signal was present in P104 myoblasts. The expression of MHC (Fig. 2C), a marker of terminal differentiation, was even observed in ΔTFT myotubes to precede that in parental myotubes, while it was undetectable in P104L myoblasts. Altogether these results suggest that while P104L mutation seems to interfere with the formation of myotubes by important attenuation of AKT pathway, as commonly characterized for both reduced differentiation and myofiber atrophy [13,14], the ΔTFT mutation confers to C2C12 myotubes an hypertrophic-like phenotype by sustained activation of AKT, a key step for developing muscle hypertrophy [15].

To next evaluate whether the increased size of ΔTFT myotubes was due to augmented myoblast recruitment, we investigated by RT-PCR analysis the expression of some specific markers such as follistatin [16], NFATC2 and IL-4 [17] (Fig. 2D), which promote myofiber growth by different mechanisms. As a long lasting increase of follistatin transcript was evident during differentiation of parental cells, both the LGMD-1C mutants exhibited significant down-regulation of follistatin expression. In addition, NFATC2 expression resulted down-regulated in P104L cells, while it appeared only slightly decreased in ΔTFT myotubes. Finally, we did not detect the expression of IL-4 nor in parental neither in LGMD-1C myoblasts at different stages of myotube formation. Therefore, the phenotypic behavior of ΔTFT cells seems to be likely due to increased AKT activation, rather than related to increased follistatin or NFATC2/IL-4 expression. Although the behavior of ΔTFT cells results elusive, it has been demonstrated that Duchenne and limb-girdle muscular dystrophies are characterized by repeated cycles of myoblast degeneration/regeneration, accompanied by hypertrophic fibers with elevated AKT signalling [18], in part confirming the main clinical features of the patients with Cav-3 deficiency, which showed mild-to-moderate proximal muscle weakness accompanied by calf hypertrophy [6]. However, it remains to establish how different mutations within Cav-3 gene have such different consequences on AKT activation.

3.2. The expression of Atrogin and Murf-1 is dysregulated in LGMD-1C myoblasts

We next focused on the expression of two muscle-specific ubiquitin ligases (E3 proteins), Atrogin/MAFbx and Murf-1 [19], whose expression is dramatically increased during cata-

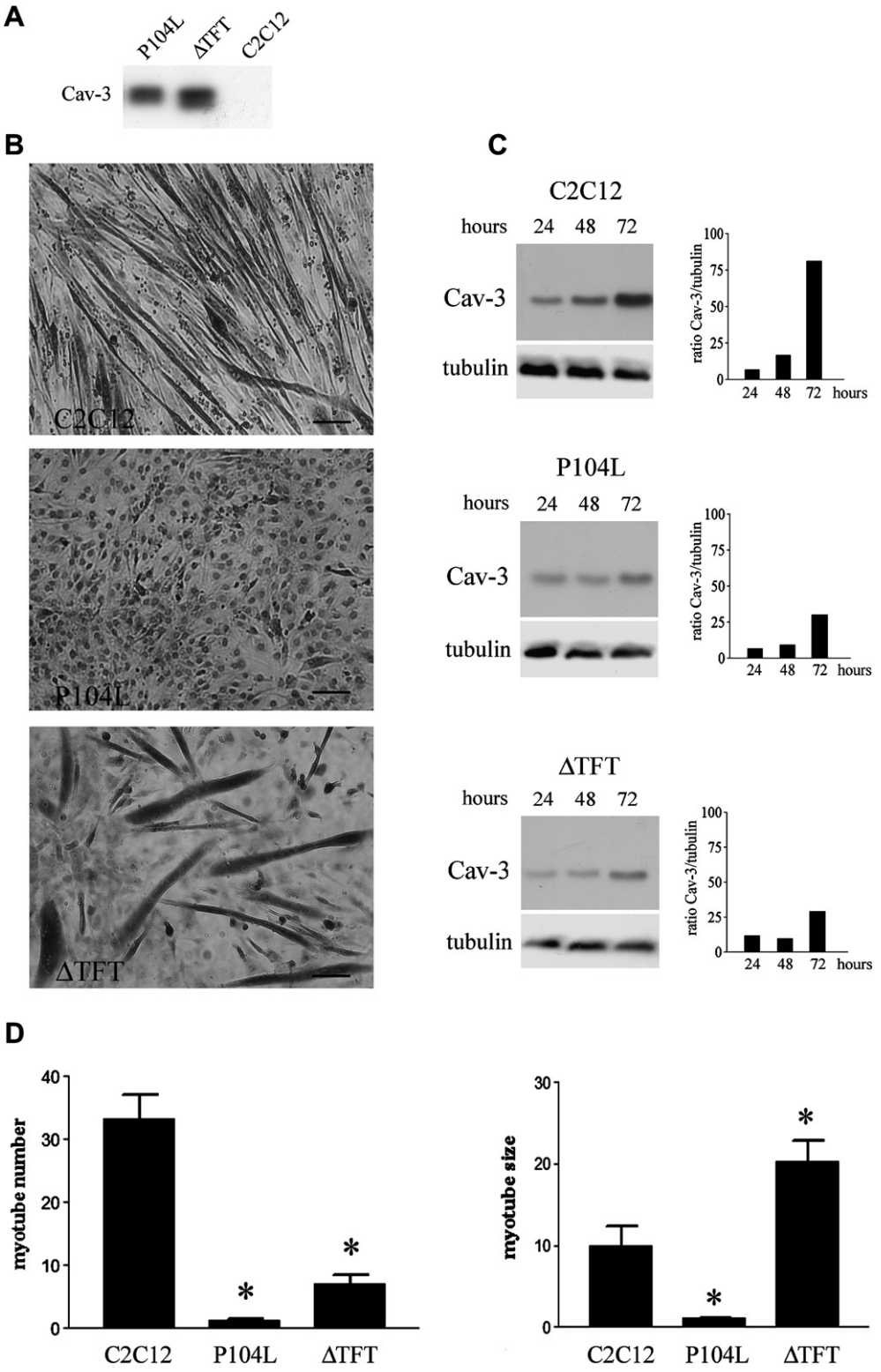

Fig. 1. Expression of P104L and ΔTFT Cav-3 related mutations affects myoblast differentiation. (A) P104L and ΔTFT transgene expression was evaluated in transfected myoblasts by Immunoblot analysis of Cav-3 expression. (B) C2C12, P104L and ΔTFT cell morphology was visualized after 72 h of differentiation. Scale bars indicate the same magnification. (C) Western blot analysis of Cav-3 expression in parental and LGMD-1C myoblasts over a time-course differentiation. The relative quantifications in the graphs were expressed as ratio between Cav-3 and tubulin expression. (D) Mean myotube number (left panel) and mean myotube size (right panel) are expressed in arbitrary units ($n = 10$, $^{*}P < 0.05$).

bolic states of muscle, triggering accelerated protein degradation via the ubiquitin-proteasome pathway [20–22]. In particular, it has been shown that P104L mutant transgenic mice display skeletal muscle atrophy due to overactivation of the

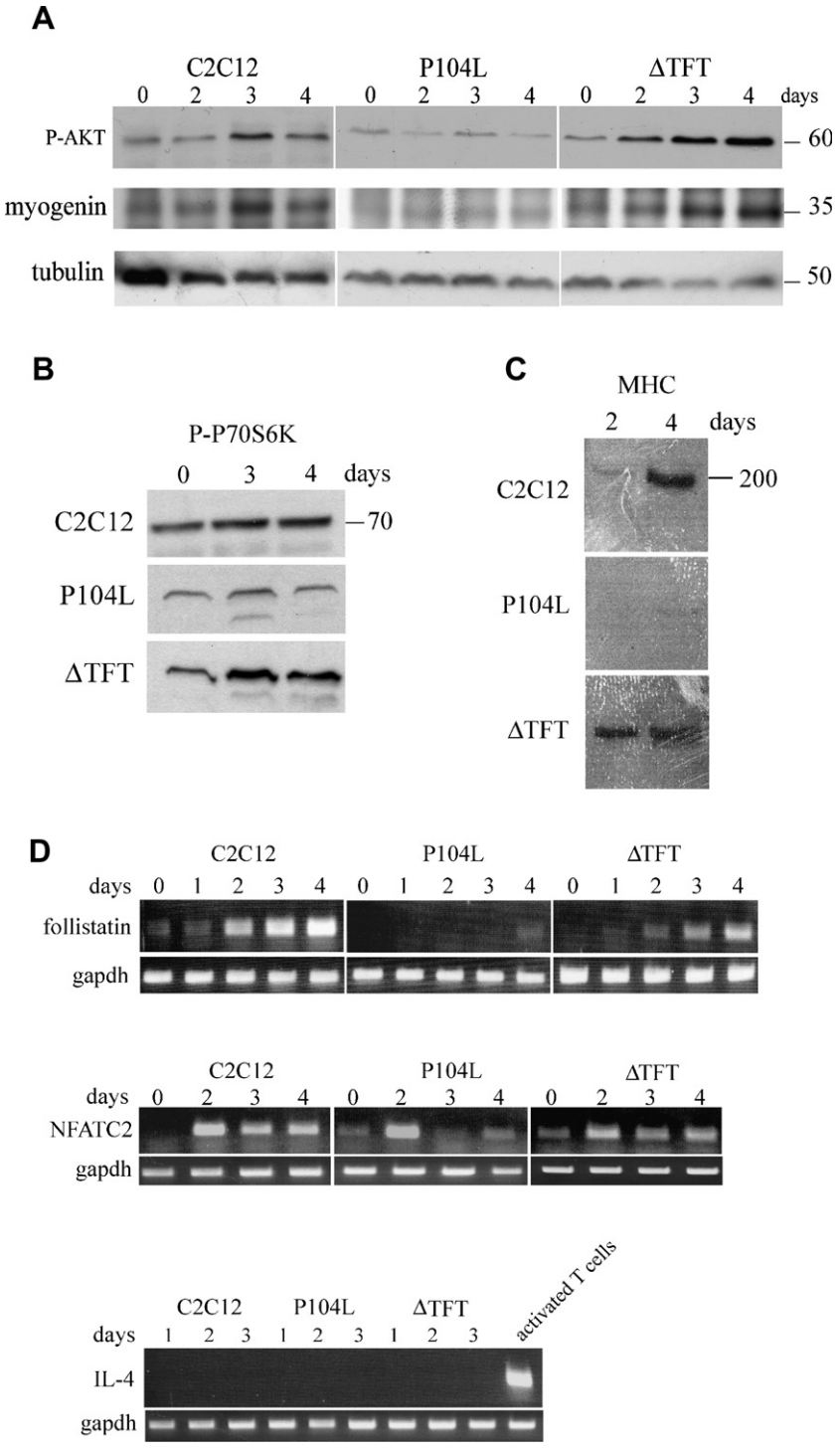

Fig. 2. Western blot analysis was performed over a 4 days time-course differentiation on C2C12 and LGMD-1C myoblasts to detect the phosphorylated AKT form and myogenin (A), the phosphorylated P70S6K form (B), and MHC (C). The data were normalized using tubulin as control. (D) RT-PCR analysis was performed over a time-course differentiation of parental and LGMD-1C myoblasts to detect the transcript profile of follistatin, NFATC2 and IL-4. Activated T lymphocytes stimulated with concanavalin A were used as positive control for 40 cycles of IL-4 amplification.

intracellular myostatin signal [9], whose essential role is to negatively regulate the skeletal muscle size [23]. Since myostatin signalling appears to antagonize the canonical hypertrophic PI3-kinase/AKT pathway, leading to activation of the ubiquitin proteolytic system [24], we performed quantitative RT-PCR analysis to detect whether the expression of Murf-1 and Atrogin would change during the defective differentiation of LGMD-1C cells (Fig. 3). While the expression of Murf-1 resulted significantly down-regulated in both LGMD-1C cells (Fig. 3A), with a more severe effect on P104L cells compared

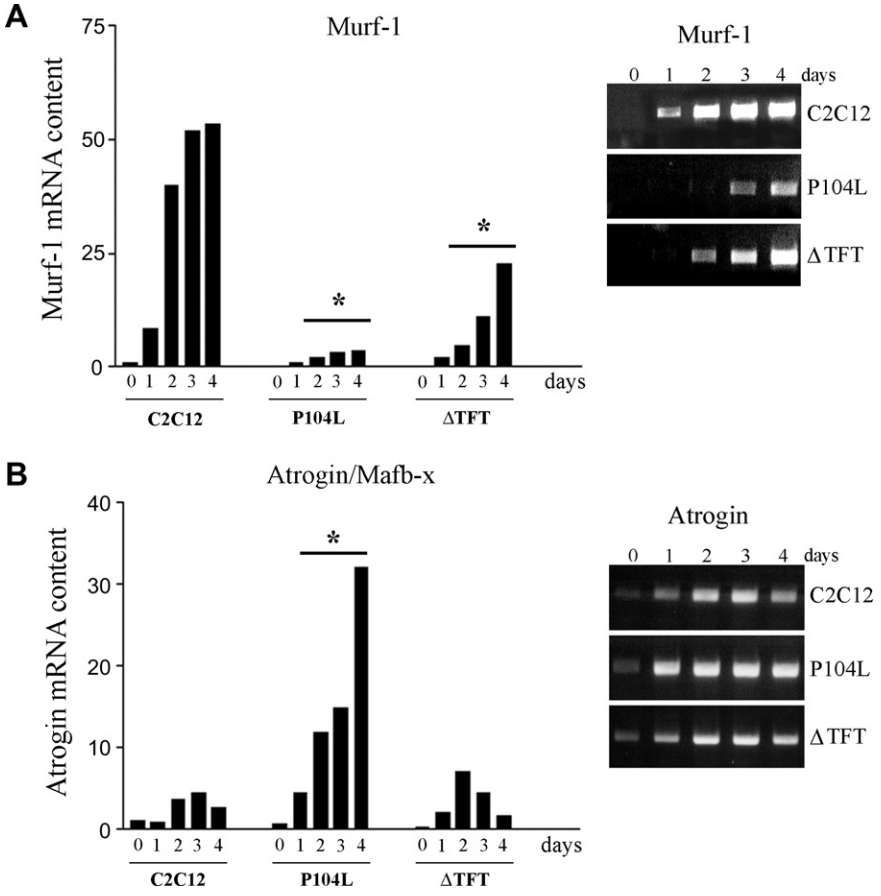

Fig. 3. Quantitative real-time PCR analysis of Murf-1 and Atrogin expression in C2C12 and LGMD-1C myoblasts. The amount of Murf-1 (A) and Atrogin (B) mRNA was analyzed by quantitative RT-PCR over a four days time-course differentiation and normalized to gapdh mRNA content ($n = 2$, $^{*}P < 0.05$). Representative semiquantitative RT-PCR are shown on the right of each graph.

to parental myoblasts, the Atrogin expression resulted dramatically up-regulated only in P104L myoblasts over the full-time course differentiation (Fig. 3B). The specific ability of P104L mutation to trigger Atrogin increase suggests that a sustained protein turn-over might impair the myofiber formation in these myoblasts, whose behavior in part reflects the phenotype of P104L mice, where enhanced myostatin signalling causes myofiber atrophy [9]. On the contrary, the ability of ΔTFT mutation to sustain the AKT signalling might preserve the cells from atrophy, leading to formation of abnormal hypertrophic myofibers. Finally, the down-regulation of Murf-1 expression in both LGMD-1C cells could represent an additional mechanism triggering myofiber degeneration, as normally the proper increase of ubiquitin ligase expression and activity contributes to myoblast differentiation, providing the required turn-over of myofibrillar proteins.

Indeed, since a clinical heterogeneity of symptoms is observed in LGMD-1C patients, our data suggest that separated mutations related to the same dystrophy associated-gene may cause muscle degeneration through distinct mechanisms, triggering different phenotypic behaviors.

Acknowledgements: We wish to thank Antonio Musarò (University of Rome) for critical reading manuscript, and Ginetta Collo (University of Brescia) for kindly providing MHC antibody. This work was supported by Grants from 60% MIUR to A.F. and to S.M. and by Grants from "Amici per il cuore" to S.M.

References

[1] Song, K.S., Scherer, P.E., Tang, Z., Okamoto, T., Li, S., Chafel, M., Chu, C., Kohtz, D.S. and Lisanti, M.P. (1996) Expression of caveolin-3 in skeletal, cardiac, and smooth muscle cells. Caveolin-3 is a component of the sarcolemma and co-fractionates with dystrophin and dystrophin-associated glycoproteins. J. Biol. Chem. 271, 15160–15165.

[2] Hnasko, R. and Lisanti, M.P. (2003) The biology of caveolae: lessons from caveolin knockout mice and implications for human disease. Mol. Interv. 3, 8445–8464, (Review).

[3] Woodman, S.E., Sotgia, F., Galbiati, F., Minetti, C. and Lisanti, M.P. (2004) Caveolinopathies: mutations in caveolin-3 cause four distinct autosomal dominant muscle diseases. Neurology 62, 538–543, Review.

[4] Galbiati, F., Volonte, D., Engelman, J.A., Scherer, P.E. and Lisanti, M.P. (1999) Targeted down-regulation of caveolin-3 is sufficient to inhibit myotube formation in differentiating C2C12 myoblasts. Transient activation of p38 mitogen-activated protein kinase is required for induction of caveolin-3 expression and subsequent myotube formation. J. Biol. Chem. 274, 30315–30321.

[5] Fanzani, A., Musaro, A., Stoppani, E., Giuliani, R., Colombo, F., Preti, A. and Marchesini, S. (2007) Hypertrophy and atrophy inversely regulate Caveolin-3 expression in myoblasts. Biochem. Biophys. Res. Commun. 357, 314–318.

[6] Minetti, C., Sotgia, F., Bruno, C., Scartezzini, P., Broda, P., Bado, M., Masetti, E., Mazzocco, P., Egeo, A., Donati, M.A., Volonté, D., Galbiati, F., Cordone, G., Bricarelli, F.D., Lisanti, M.P. and Zara, F. (1998) Mutations in the caveolin-3 gene cause autosomal dominant limb-girdle muscular dystrophy. Nat. Genet. 18, 365–368.

[7] Galbiati, F., Volonte, D., Minetti, C., Bregman, D.B. and Lisanti, M.P. (2000) Limb-girdle muscular dystrophy (LGMD-1C)

mutants of caveolin-3 undergo ubiquitination and proteasomal degradation. J. Biol. Chem. 275, 37702–37711.
[8] Sunada, Y., Ohi, H., Hase, A., Ohi, H., Hosono, T., Arata, S., Higuchi, S., Matsumura, K. and Shimizu, T. (2001) Transgenic mice expressing mutant caveolin-3 show severe myopathy associated with increased nNOS activity. Hum. Mol. Genet. 10, 173–178.
[9] Ohsawa, Y., Hagiwara, H., Nakatani, M., Yasue, A., Moriyama, K., Murakami, T., Tsuchida, K., Noji, S. and Sunada, Y. (2006) Muscular atrophy of caveolin-3-deficient mice is rescued by myostatin inhibition. J. Clin. Invest. 116, 2924–2934.
[10] Nixon, S.J., Wegner, J., Ferguson, C., Mery, P.F., Hancock, J.F., Currie, P.D., Key, B., Westerfield, M. and Parton, R.G. (2005) Zebrafish as a model for caveolin-associated muscle disease; caveolin-3 is required for myofibril organization and muscle cell patterning. Hum. Mol. Genet. 14, 1727–1743.
[11] Smythe, G.M., Eby, J.C., Disatnik, M.H. and Rando, T.A. (2003) A caveolin-3 mutant that causes limb girdle muscular dystrophy type 1C disrupts Src localization and activity and induces apoptosis in skeletal myotubes. J. Cell Sci. 116, 4739–4749.
[12] Smythe, G.M. and Rando, T.A. (2006) Altered caveolin-3 expression disrupts PI(3) kinase signaling leading to death of cultured muscle cells. Exp. Cell Res. 312, 2816–2825.
[13] Bodine, S.C., Stitt, T.N., Gonzalez, M., Kline, W.O., Stover, G.L., Bauerlein, R., Zlotchenko, E., Scrimgeour, A., Lawrence, J.C., Glass, D.J. and Yancopoulos, G.D. (2001) Akt/mTOR pathway is a crucial regulator of skeletal muscle hypertrophy and can prevent muscle atrophy in vivo. Nat. Cell Biol. 3, 1014–1019.
[14] Peng, X.D., Xu, P.Z., Chen, M.L., Hahn-Windgassen, A., Skeen, J., Jacobs, J., Sundararajan, D., Chen, W.S., Crawford, S.E., Coleman, K.G. and Hay, N. (2003) Dwarfism, impaired skin development, skeletal muscle atrophy, delayed bone development, and impeded adipogenesis in mice lacking Akt1 and Akt2. Genes Dev. 17, 1352–1365.
[15] Lai, K.M., Gonzalez, M., Poueymirou, W.T., Kline, W.O., Na, E., Zlotchenko, E., Stitt, T.N., Economides, A.N., Yancopoulos, G.D. and Glass, D.J. (2004) Conditional activation of akt in adult skeletal muscle induces rapid hypertrophy. Mol. Cell Biol. 24, 9295–9304.
[16] Iezzi, S., Di Padova, M., Serra, C., Caretti, G., Simone, C., Maklan, E., Minetti, G., Zhao, P., Hoffman, E.P., Puri, P.L. and Sartorelli, V. (2004) Deacetylase inhibitors increase muscle cell size by promoting myoblast recruitment and fusion through induction of follistatin. Dev Cell. 6, 673–684.
[17] Horsley, V., Jansen, K.M., Mills, S.T. and Pavlath, G.K. (2003) IL-4 acts as a myoblast recruitment factor during mammalian muscle growth. Cell 113, 483–494.
[18] Peter, A.K. and Crosbie, R.H. (2006) Hypertrophic response of Duchenne and limb-girdle muscular dystrophies is associated with activation of Akt pathway. Exp. Cell Res. 312, 2580–2591.
[19] Bodine, S.C., Latres, E., Baumhueter, S., Lai, V.K., Nunez, L., Clarke, B.A., Poueymirou, F.J., Panaro, E.Na.K., Dharmarajan, Z.Q., Pan, D.M., Valenzuela, T.M., DeChiara, W.T., Stitt, T.N., Yancopoulos, G.D. and Glass, D.J. (2001) Identification of ubiquitin ligases required for skeletal muscle atrophy. Science 294, 1704–1708.
[20] Gomes, M.D., Lecker, S.H., Jagoe, R.T., Navon, A. and Goldberg, A.L. (2001) Atrogin-1, a muscle-specific F-box protein highly expressed during muscle atrophy. Proc. Natl. Acad. Sci. USA 98, 14440–14445.
[21] Lecker, S.H., Jagoe, R.T., Gilbert, A., Gomes, M., Baracos, V., Bailey, J., Price, S.R., Mitch, W.E. and Goldberg, A.L. (2004) Multiple types of skeletal muscle atrophy involve a common program of changes in gene expression. FASEB J. 18, 39–51.
[22] Sandri, M., Sandri, C., Gilbert, A., Skurk, C., Calabria, E., Picard, A., Walsh, K., Schiaffino, S., Lecker, S.H. and Goldberg, A.L. (2004) Foxo transcription factors induce the atrophy-related ubiquitin ligase atrogin-1 and cause skeletal muscle atrophy. Cell 117, 399–412.
[23] McPherron, A.C., Lawler, A.M. and Lee, S.J. (1997) Regulation of skeletal muscle mass in mice by a new TGF-beta superfamily member. Nature 387, 83–90.
[24] McFarlane, C., Plummer, E., Thomas, M., Hennebry, A., Ashby, M., Ling, N., Smith, H., Sharma, M. and Kambadur, R. (2006) Myostatin induces cachexia by activating the ubiquitin proteolytic system through an NF-kappaB-independent, FoxO1-dependent mechanism. J. Cell Physiol. 209, 501–514.